

Electronic band structure of nitrogen diluted Ga(PAsN)

Electronic band structure of nitrogen diluted Ga(PAsN): formation of the intermediate band, direct and indirect optical transitions, localization of states

M. P. Polak,^{1, a)} R. Kudrawiec,¹ and O. Rubel²

¹⁾*Department of Experimental Physics, Faculty of Fundamental Problems of Technology, Wroclaw University of Science and Technology, Wyb. Wyspianskiego 27, 50-370 Wroclaw, Poland*

²⁾*Department of Materials Science and Engineering, McMaster University, 1280 Main Street West, Hamilton, Ontario L8S 4L8, Canada*

(Dated: 20 September 2019)

The electronic band structure of Ga(PAsN) with a few percent of nitrogen is calculated in the whole composition range of Ga(PAs) host using density functional methods including the modified Becke-Johnson functional to correctly reproduce the band gap, and unfolding of supercell band structure to reveal the character of the bands. Relatively small amounts of nitrogen introduced to Ga(PAs) lead to formation of an intermediate band below the conduction band which is consistent with the band anticrossing model, widely used to describe the electronic band structure of dilute nitrides. However, in this study calculations are performed in the whole Brillouin zone and reveal the significance of correct description of band structure near the edges of Brillouin zone, especially for indirect band gap P-rich host alloy, which may not be properly captured with simpler models. The influence of nitrogen on the band structure is discussed in terms of application of Ga(PAsN) in optoelectronic devices such as intermediate band solar cells, light emitters as well as two colour emitters. Additionally, the effect of nitrogen incorporation on the carrier localization is studied and discussed. The theoretical results are compared with experimental studies, confirming their reliability.

^{a)}M. P. Polak: maciej.polak@pwr.edu.pl

Electronic band structure of nitrogen diluted Ga(PAsN)

I. INTRODUCTION

Nitrogen diluted III-V alloys are compelling to study for many reasons including the anticrossing interaction the in conduction band¹, an enhanced conduction band non-parabolicity², or carrier localization phenomena^{3,4}. One feature of these alloys makes them very unusual among other III-V alloys and thereby very interesting in applied physics, i.e. a simultaneous reduction of the band gap and the lattice constant due to the incorporation of nitrogen into the III-V host. This feature makes dilute nitrides promising for extending the emission of GaAs and InP-based lasers to longer wavelengths⁵⁻⁷ and desired light absorbers in multijunction solar cells⁸⁻¹⁰. In addition, dilute nitrides can be utilized as absorbers in intermediate band solar cells (IBSC), which have been proposed by Luque and Marti¹¹ for obtaining high-efficiency single junction solar cells¹².

In recent years the concept of IBSC has been very intensively explored. Nowadays it is generally accepted that the intermediate band absorbers can be divided into three large groups: nanostructures, such as quantum dots¹³⁻¹⁵, semiconductor bulk materials containing a high density of deep-level impurities^{13,14,16}, and highly mismatched alloys (HMAs) i.e., semiconductor alloys where the band anticrossing (BAC) effect takes place^{1,17,18} and an intermediate band is formed.

Among HMAs, Ga(PAsN) with ~40% P and a few percent of nitrogen has been recognized as the most optimal for application in IBSCs¹⁸. Therefore in recent years this alloy has been intensively explored¹⁹⁻²². Moreover, Ga(PAsN) alloys with P concentration greater than 60% have also been studied²³⁻²⁶. This range of P concentration in Ga(PAsN) alloy seems to be the most interesting from the viewpoint of intermediate band formation and lattice matching with Si platform²⁶. The possible integration of Ga(PAsN) with Si platform is a very important advantage of this alloy, which also makes this material system very promising for laser applications. For these purposes As-rich Ga(PAsN) alloys and quantum wells with a few percent of nitrogen atoms have been studied^{27,28} and an electrically pumped laser on Si platform with the active region containing Ga(PAsN) quantum well has been demonstrated²⁹. However further application of Ga(PAsN) alloy in IBSCs and lasers integrated with Si platform needs better understanding of the electronic band structure of this alloy in the full Brillouin zone. It includes the understanding of formation of the intermediate band, the role of localized and delocalized states, as well as the character of host band gap (direct vs indirect) with the change in the content of Ga(PAsN) alloy.

Electronic band structure of nitrogen diluted Ga(PAsN)

To explain the composition dependence of the band gap in Ga(PAsN) the band anti-crossing (BAC) model is very often utilized^{18–21}. This model has been developed in order to describe changes in the band gap of HMAs, which due to high electronic and size mismatch could not be properly characterized with virtual crystal approximation (VCA), traditionally used for regular semiconductor alloys³⁰. According to the BAC model the interaction of dispersionless N-related states with conduction band states of Ga(PAs) host is modelled as a two-level system by the following Hamiltonian^{1,31}

$$H_{BAC} = \begin{bmatrix} E_M(k) & C_{NM}\sqrt{x} \\ C_{NM}\sqrt{x} & E_N \end{bmatrix} \quad (1)$$

where x is the mole fraction of substitutional N atoms and C_{NM} is a coupling parameter which describes the interaction between the nitrogen level and the conduction band. This parameter depends on the semiconductor matrix and can be determined experimentally^{1,18}. $E_M(k)$ is the energy dispersion of the lowest conduction band of the III-V matrix and E_N is the energy of N-related states, all referenced to the top of the valence band. Eigenvalues $E_-(k)$ and $E_+(k)$ of the Hamiltonian (1) form two highly non-parabolic subbands. The E_- band has features of a narrow intermediate band (IB) and is well separated by an energy gap from the E_+ band, i.e., the upper conduction band (CB), at the Γ -point. This gap is one of the subjects of studies in this work since its existence throughout the *entire* Brillouin zone (BZ) is very important for the application of Ga(PAsN) as an IB absorber in IBSCs.

A HMA absorber in IBSC should utilize three bands resulting in the optical transitions from VB to CB ($\Gamma_v - E_+$ band), from VB to IB ($\Gamma_v - E_-$ band), and IB to CB, as schematically shown in Fig. 1. An optimal total band gap of the IBSC should be 1.95 eV (100%) split in the ratio of approximately 36%/64% between the two optical transitions $E_- - E_+$ and $\Gamma_v - E_-$ ³². It is favourable for the CB to show a slight indirect character to scatter electrons from Γ valley and prolong their lifetime. In order to suppress carrier relaxation from CB to IB (i.e., to fulfil the condition necessary for an efficient IBSC operation) these bands have to be separated by an energy gap in the *whole* BZ¹¹. Such a separation exists within the BAC model, but is confirmed experimentally only at the *center* of the Brillouin zone by modulation spectroscopy^{1,18} since this technique probes only direct optical transitions^{1,18}. Therefore the question of existence of an energy gap between IB and CB in Ga(PAsN) and other HMAs is still open.

A combination of the $\mathbf{k}\cdot\mathbf{p}$ and BAC model is a popular choice for modelling of the band structure of HMAs^{6,7,33}. However, the model applies only to electronic states in vicinity of

Electronic band structure of nitrogen diluted Ga(PAsN)

Γ point and ignores the disorder in IB, e.g. the degree of localization of electronic states, which is responsible for inhomogeneous broadening of luminescence spectra and gain spectra in lasers. Extending the conclusions drawn from the BAC and $\mathbf{k}\cdot\mathbf{p}$ approach to the electronic band structure in the full BZ is very interesting^{18,34}, but can be controversial because of the limitations of the $\mathbf{k}\cdot\mathbf{p}$ method. Therefore, proper modelling of the electronic band structure of Ga(PAsN) in the full BZ is very important when considering the application of this alloy in IBSC as well as other devices. So far the electronic band structure of ternary Ga(AsN) and Ga(PN) alloys (i.e., extreme host content cases of Ga(PAsN)) has been calculated using empirical pseudopotential^{35,36}, tight-binding methods³⁷, and density functional theory (DFT) approaches^{38,39} but the issue of IB formation and the energy separation between the IB and the CB as well as the degree of localization of electronic states was not addressed. The quaternary dilute nitride Ga(PAsN) have also not been previously studied by DFT methods in the full composition range.

The aim of this paper is to computationally obtain the electronic band structure using DFT based methods for Ga(PAsN) alloy in the whole BZ (not only in the vicinity of the Γ point, as it is commonly done within the BAC model) and for a full composition range of Ga(PAs) host. The resultant electronic band structures are then discussed in the context of application of Ga(NPAs) in IBSC and light emitters including the concept of two color emitters recently proposed for HMAs⁴⁰. For this purpose we applied state-of-the-art DFT methods, utilizing large supercells in order to study hundreds of different compositions on dense composition grids together with the band unfolding technique based on spectral weights^{41,42}. It allows to obtain an effective band structure of a solid solution from folded supercell bands giving the possibility of distinguishing between direct and indirect gaps as well as provides insight into the Bloch character of bands. To investigate the degree of localization of electronic states, an inverse participation ratio method⁴³ has been applied. Since the main subject of this study is the quaternary Ga(PAsN) alloy, for additional credibility and broader extent and analysis of the results, all directly related ternary alloys have been studied using the same method as well, i.e. the Ga(PAs) host in the whole composition range, and the Ga(PN) and Ga(AsN) alloys with N content limited up to around 10% due to challenges associated with their synthesis. This resulted in an extensive, consistent and comprehensive study of a whole family of systems, allowing for direct and reliable comparison of the calculated quantities between them.

II. COMPUTATIONAL METHODS

The first-principles calculations have been carried out using density functional theory^{44,45} and the linear augmented plane wave method implemented in the WIEN2k package⁴⁶. The SCAN functional⁴⁷ has been used to capture exchange-correlation effects in the geometry optimization. The modified Becke-Johnson exchange potential (mBJ)⁴⁸ combined with the local density approximation (LDA) for correlation⁴⁹ has been used in the band structure calculations to obtain realistic band gaps, with accuracy comparable to hybrid functionals⁵⁰ or the GW approach and considerably lower computational cost^{51–53}. Even though mBJLDA significantly improves over standard DFT semi-local exchange-correlation functionals in the description of band gaps, the c parameter of the mBJLDA functional (Eq. 3 in⁴⁸) allows for some fine tuning of the band gap if needed. Therefore, we slightly adjusted the c parameter to achieve a perfect agreement of the calculated direct band gaps with experimental (0 K) values for the parent binary compounds, since they are a starting point of all following calculations. It is a standard practice, similar to the adjustment of the α parameter, a fraction of exact exchange, in hybrid HSE functionals, and allows for easier comparison with experimental measurements and prediction of subsequent properties. Table I presents a comparison of our results for the band gaps with experimental values and lists the adjusted values of the c parameter.

Solid solutions have been simulated via constructing 128-atom supercells by translating the 2-atom basis along the primitive lattice vectors of the zinc-blend structure with a multiplicity of $4 \times 4 \times 4$. A consistent way of distributing different elements within the supercell has been achieved by generating special quasirandom structures (SQS)⁵⁴ with the use of the `mcsqs` code⁵⁵. Quadruplets and triplets with the closest neighbor of the same kind as well as pairs to three closest neighbors have been considered for correlation functions, and the Monte Carlo algorithm has been run for $3 \cdot 10^6$ iterations which has been found to be sufficient to either find a perfect match or for an objective function to converge.

Radii R of muffin-tin spheres of As, Ga, P and N has been chosen to be 2.2, 2.2, 1.9 and 1.7 a.u. respectively. Considering the small muffin-tin sphere of the nitrogen atom and the size of a 128-atom supercell, convergence studies lead to a $R_{\min}K_{\max} = 7$ for nitrogen-containing structures. The increased value of $R_{\min}K_{\max} = 7.5$ was used for nitrogen-free $\text{GaP}_{1-x}\text{As}_x$ structures. The BZ of supercells was sampled with a Monkhorst-Pack mesh⁵⁶ of $2 \times 2 \times 2$ (equivalent to $8 \times 8 \times 8$ in the primitive zinc blende unit cell).

Electronic band structure of nitrogen diluted Ga(PAsN)

Lattice parameters and the *c*-mBJLDA parameters of alloys were interpolated from binary solids, which has been proven to be successful in previous studies of similar systems^{57,58}. Then, full optimization of internal ionic degrees of freedom has been performed until the maximum forces acting on a single atom did not exceed 1 mRy/Bohr with a force convergence of 0.1 mRy/Bohr. In the band structure and density of states (DOS) calculations, energy convergence of 1 mRy was used. For the DOS calculations in 128-atom supercells (Fig. 8), which have been crucial in determining the intermediate gap, a much denser k mesh of $8 \times 8 \times 8$ (equivalent to $32 \times 32 \times 32$ in the primitive zinc blende unit cell) has been used together with an improved tetrahedron method⁵⁹ to achieve a better energy resolution and avoid false conclusions.

Considering the difficulties in interpretation of band structures of supercells, especially in materials with an indirect band gap (GaP), as well as the formation of the intermediate band, the band unfolding technique described in Refs. 41,42 and implemented in the `fold2Bloch` code⁶⁰ has been used. The code computes spectral weights $w_n(\mathbf{k})$ in the range 0–1 for each n 's energy eigenstate to reflect its Bloch \mathbf{k} character. The number of spectral weights computed per eigenstate corresponds to the multiplicity of the supercell (64 in this case). The approach to the calculation of spectral weights is based on remapping the supercell reciprocal space with a mesh that is compatible with the translational symmetry of a primitive cell. Computed Bloch spectral weights for each eigenstate in a supercell calculation fulfill the normalization $\sum_{\mathbf{k}} w_n(\mathbf{k}) = 1$, which implies that the cumulative probability of finding an electron in any of multiple \mathbf{k} 's states adds up to one. Further details of the method and implementation can be found elsewhere^{41,42,60}.

III. RESULTS AND DISCUSSION

A. Formation of the intermediate band

As emphasized in Sec. I, the properly calculated and unfolded DFT band structures provide us with a complete, whole BZ picture of the energy band dispersions. This is particularly useful when the host material has an indirect gap, as in Ga(PAs), up to around 51% of its As composition range on the P rich side.

Figure 2 (a)-(f) shows the unfolded band structures of six compositions of the $\text{GaP}_{1-x}\text{As}_x$ alloy, which will serve as a reference for Ga(PAsN). The unfolded band structures throughout

Electronic band structure of nitrogen diluted Ga(PAsN)

the whole composition range consist of eigenvalues with high Bloch spectral weights, mostly over 80% at the band edges. This material is well known experimentally⁶¹, and its excellent optical properties have lead to its frequent use in light emitting diodes or multi-junction III-V solar cells. Those high spectral weights are due to the similarity of size and electronegativity between P and As atoms, and directly relate to the good optical quality of the material and a very low amount of localized states, which is discussed later in Sec. III B.

Figure 3 shows the energies of direct and indirect gaps as well as the spin-orbit split off band gap in Ga(PAs). The points represent the values of energy gaps obtained from band edges of unfolded band structures and the lines are second order polynomial fits according to the Vegard's law with a constant bowing parameter b :

$$E_g^{AB_{1-x}C_x} = (1 - x)E_g^{AB} + xE_g^{AC} - bx(1 - x) \quad (2)$$

where E_g is the band gap and x is the fractional composition. This is the widely used approximation of the composition dependence of the band gap used for regular semiconductor alloys.

The distinction between direct and indirect gaps has been enabled due to the band unfolding and is otherwise obstructed by zone folding in supercell calculations. It is important to notice that the lines in Fig. 3 provide a nearly perfect fit to the obtained data points. The scattering of $E_g(x)$ values is very small even near to the middle of the composition range. This behaviour is a consequence of a well-preserved Bloch character at the band edges. It is also a characteristic of an alloy without substantial localization of states resulting in desirable transport properties that is crucial for solar cell absorber materials. This good applicability of the parabolic Vegard's law is also characteristic of ordinary, well matched semiconductor alloys.

Materials with lower metallicity and higher polarity, such as GaP, tend to have higher and indirect band gaps, and for higher metallicity and lower polarity, such as GaAs, band gaps are smaller and more direct⁶². Therefore when alloying GaP with GaAs, the metallicity increases (and the polarity decreases), driving the change in the band gap character from indirect to direct. The crossover is anticipated at 54% of As content for a linear interpolation of the band gaps as a function of composition (i.e., a rule of mixture of two materials). More accurate electronic structure calculations suggest the intersection of $\Gamma_v - \Gamma_c$ and $\Gamma_v - X_c$ gaps, i.e., the indirect-direct transition in Fig. 3, to occur at around 51% of As content, which is concurrent with experimental observations⁶¹. The discrepancy is due to an additional

Electronic band structure of nitrogen diluted Ga(PAsN)

bowing of band gaps [parameter b in Eq. 2]. The physical origin of the bowing of band gaps is related to clustering effects⁶³, which becomes more prominent in highly mismatched alloys. The bowing parameter for the direct band gap is $b = 0.33$ eV (Table II), which is close to the bowing parameter $b = 0.19$ eV recommended by Vurgaftman et al.⁶¹. This small difference can be attributed to a finite temperature at which the experimental parameter has been obtained in contrast to our 0 K calculations as well as other experimental factors not accounted for in the modelling. The discrepancy results in a maximum error of 35 meV for the band gap at $x = 0.5$ of this alloy and smaller differences at other alloy contents. Therefore it can be assumed that our theoretical predictions are consistent with previous studies of this alloy⁶¹ and ensure a solid starting point for calculations of the alloys with nitrogen.

Before proceeding to the quaternary Ga(PAsN) alloy, it is worth establishing that properties of the ternary alloys Ga(PN) and Ga(AsN) can also be reproduced. Figure 2 (g) and (m) show the unfolded band structures for the Ga(PN) alloy in the dilute N regime. This material is one of the key representatives of HMAs, and its behavior is expected to be much different from an ordinary semiconductor alloy such as the previously discussed Ga(PAs). For the low nitrogen content, a clearly visible intermediate band is formed. A decomposition of the DOS on different atoms and their orbitals reveals that the part of the DOS corresponding energetically to the intermediate band consists primarily of N-s states, which has been expected from the BAC model.

It is difficult to confidently establish from the band structure alone a composition limit in which the energy gap between the nitrogen-induced IB and the host conduction band exists. The existence of this gap is an important ingredient for IBSC absorber materials (Fig. 1). For the lowest available composition in our 128-atom supercell, i.e. 1.56% of N, the band structure suggest that a presence of such gap is possible (Fig. 2 (g)), but as the nitrogen content increases, the gap seems to be closing. This behavior can be attributed to the change in the dispersion of the nitrogen intermediate band, which changes from relatively flat for spatially isolated N atoms to a more parabolically curved band when more atoms are introduced and their s-states interact as the spatial separation is reduced. The gap can be properly identified on a well-resolved DOS constructed using a dense k mesh, which is done for the Ga(PAsN) alloy (Fig. 8) and will be discussed later.

The energies of direct optical transitions inferred from unfolded band structures of $\text{GaP}_{1-x}\text{N}_x$ with $x < 0.11$ are shown in Fig. 4. The high mismatch in electronegativity and

Electronic band structure of nitrogen diluted Ga(PAsN)

size between P and N atoms, which allows to categorize this material as HMA, limits the applicability of the standard parabolic equation for the composition dependence of the band gaps [Eq. (2)], since the composition dependence of the band gap in this type of alloys tends to be non-parabolic. Instead, the BAC model is used [Eq. (3)] with parameters listed in Table II

$$\begin{aligned} E_{\pm}(k) = \\ = \frac{1}{2} \left\{ E_M(k) + E_N \pm \sqrt{[E_M(k) - E_N]^2 + 4 [C_{NM}(k)]^2 x} \right\} \end{aligned} \quad (3)$$

As a result of calculating the band structure within the whole BZ, a modification of the host conduction band due to the introduction of nitrogen can be studied not only in the Γ point but also in the L - and X -points. The energy levels at the L and X points are affected less than at Γ , which reflects in lower values of the corresponding coupling parameters $C_{NM}(k)$ (Table II). Higher N-concentrations distort the host CB much more, yet still affect the center of the BZ the most. According to our DFT calculations the *s*-like character of the conduction band in GaP host is weaker at the end of BZ (100% at the Γ point as opposed to 78% and 36% at the L-point and X-valley, respectively) and therefore the $C_{NM}(k)$ element is smaller at the end of BZ. This agrees with the experimental results from⁶⁴, where the BAC interaction is found to be k -vector dependent, and its strength decreases away from the center of the BZ.

A very similar discussion of the band structure can be held for Ga(AsN), where a nitrogen band in a low concentration regime is visible on the unfolded band structures as well [Fig. 2 (l) and (r)]. Here, however, due to the smaller band gap and an energetically lower position of the conduction band of the host GaAs, the curvature of the intermediate band is more pronounced and the IB overlaps with the conduction band, eliminating the possibility of the material to have a well defined intermediate gap between the two bands (Fig. 1). The relatively closer proximity of the N states comprising the IB allow for them to interact more with the conduction band states of the host's CB and even in the case of low N composition and N atoms isolated from each other, the higher curvature of the band is possible.

The energies of direct and indirect optical transitions obtained from unfolded band structures of $\text{GaAs}_{1-x}\text{N}_x$ with $x < 0.11$ are shown in Fig. 5. In this case, if the CB is split into two bands [Fig. 2 (l)] the lower spectral weight eigenvalue seems to follow the BAC curve much better. This splitting is shown in Fig. 5 as filled and open red squares. This artefact may result from a limited size of the supercell and periodic boundary conditions which does

Electronic band structure of nitrogen diluted Ga(PAsN)

not allow for a perfectly uniform N atom distribution, due to which unintended clustering or isolation of atoms may occur, resulting in split states. The wave-vector dependence of the coupling parameters $C_{NM}(k)$ has the same character as in GaP host, due to the similar k -vector dependence of the *s*-like character of the conduction band, although the magnitude of the dependence is different. In general, different k -vector dependence of the coupling parameter should be expected for different III-V hosts due to the different orbital structure and wavefunction character of the bands when moving from the center to the end of the BZ.

The intermediate band behaviour of Ga(PN) and Ga(AsN) combined with the possibility of the band gap tuning of Ga(PAs) as well as a possible integration with the Si platform by matching the lattice parameters suggests that a ternary alloy might be a good candidate for solar cell application, especially in a very low nitrogen content on the P-rich side of the Ga(PAsN) alloy, where the desirable intermediate gap is likely to be observed.

Following these assumptions, an electronic band structure of the Ga(PAsN) alloy was studied for two lowest nitrogen concentrations, namely 1.56% and 3.12%, and a whole P/As composition range. Taking into account the fact that results of our effective band structure calculations match the experimental trends as well as the BAC model for the well known Ga(PAs) and low nitrogen concentration Ga(PN) and Ga(AsN) alloys, we expect that the methods used here should give reliable results for the band structure of the Ga(PAsN) alloy.

The effective band structures for selected compositions are presented in Fig. 2(n)–(p). As expected, the addition of nitrogen resulted in splitting of the conduction band into two E_- and E_+ subbands. The character of the disorder in the band structure changes with the variation in composition of the host, due to the change in mismatch in electronegativity and size between the host's P/As atoms and nitrogen, as well as their different electronic structures. As a consequence, states at the bottom of the IB become progressively more Γ -like as the composition shifts toward the As-rich limit. The IB is always clearly visible and distinguishable.

A composition dependence of direct and indirect optical transitions in Ga(PAsN) alloys is presented in Fig. 6. Some important findings can be extracted from this figure. Treating the E_- band as the IB and E_+ band as the CB it is interesting to analyse the minimum of CB since Ga(PAsN) alloys with the energy minimum at the Γ point are potential candidates for two colours emitters. For such emitters the radiative recombination takes place at the Γ point of BZ from the CB to the VB and from the IB to the VB. The channel of recombination between the IB and the VB is expected in the whole range of Ga(PAsN) content since the

Electronic band structure of nitrogen diluted Ga(PAsN)

minimum of IB is at the Γ point. Electrons easily thermalize to this state and recombine radiatively with holes. The energy minimum in CB varies depending on the content of Ga(PAsN) alloy. For Ga(PAsN) alloy with low N concentration [Fig. 6 (a)] the order of the Γ , X and L energy position is similar to that observed in Ga(PAs) host, see Fig. 3. In this case the minimum of CB is at the Γ point for As-rich Ga(PAsN) alloys only. With the increase in N concentration this order in the CB is no longer present, see Fig. 6 (b). For Ga(PAsN) alloys with the energy minimum in E_+ band outside of the Γ point (i.e., at the X or L point) carriers can thermalize outside the center of BZ and cannot recombine radiatively since holes thermalize to the Γ point. Such conditions are present for P-rich Ga(PAsN) alloys and enhance with the increase in N concentration.

The other feature extracted from Fig. 6 is that the energy separation between the IB and the CB at the Γ point changes very weakly with the content of Ga(PAs) host while the energy difference between the VB and the IB changes almost twice in the full content range. This behavior can be attributed to the fact that the majority of the band gap reduction comes from the valence band, governed mostly by group V elements, while the localized nitrogen level remains fixed in energy. Such features of the electronic band structure can be utilized in band gap engineering in semiconductor devices.

As will be shown later, the nitrogen-related states are highly localized and, hence, the energy eigenvalues in calculations are highly dependent on the nitrogen atom distribution. The 1.56% N-composition corresponds to only one atom in a 128 atom supercell which creates an ordered distribution of nitrogen atoms within the host Ga(PAs). This results in relatively smooth composition-dependent $E_g(x)$ curves, with a small scattering of the points caused only by alloy fluctuations of the host Ga(PAs) atoms in our calculations, see Fig. 6 (a).

In the case of 3.12% N-content, there are two atoms in the supercell distributed by the SQS algorithm together with the host Ga(PAs) atoms. A dense composition grid resulting from the use of relatively large quasi-randomly populated supercells allows to observe variation of the distance between the two N-atoms results in a much higher scattering of the points, see Fig. 6 (b). The scattering of data for E_- in Fig. 6 (b) provides an estimate of 0.1 eV for the energy scale of inhomogeneous broadening due to N-N configurational fluctuations. Limitations imposed by the size of the supercell and dilute N-content preclude us from investigating triplets and higher order N-clusters. Those details can be found elsewhere⁶⁵.

In order to provide an easy way of estimating the energy of $\Gamma - E_{\pm}$ transitions as well

Electronic band structure of nitrogen diluted Ga(PAsN)

as E_+ energies in L and X points for different compositions of the Ga(PAsN) alloy with low nitrogen content (x up to around 0.10 and $T = 0$ K) we have combined all of the results of the changes in energies as a function of composition and derived an approximate general formulas for E_{\pm} . The expression is based on Eq. (2) for Ga(PAs), where the values of E_g^{AB} and E_g^{AC} are calculated with the use of Eq. (1) for Ga(PN) and Ga(AsN) respectively. The C_{NM} and E_N parameters were linearly interpolated between Ga(PN) and Ga(PAs) (see Table II). It is worth noticing, that although the $C_{NM}(\Gamma)$ and E_N parameters for both Ga(PN) and Ga(AsN) can be extracted from the results, well established and commonly used experimental parameters have been used^{66,67}. The parameters outside of the Γ point, however, have not been determined before, therefore the values extracted from our calculations are used, creating the possibility for a complete description of the band edge energies within the whole BZ.

We validate the model equations by comparing calculated energies of direct optical transitions in the Ga(PAsN) alloy with those determined experimentally. Figure 7 shows experimental points from Ref.²⁶ obtained at room temperature as a function of As concentration together with our theoretical predictions for N = 2.5 % and shifted by 100 meV, which accounts for the temperature shift of the band gap in this alloy between 0 and 300 K. As seen in Fig. 7 the agreement between experimental data and our predictions is very good for both the E_- and E_+ transition. It confirms that our calculations are reliable and satisfactorily describe the electronic band structure of this alloy.

In a search for a gap between the IB and the host conduction band, we inspected the DOS of Ga(PAsN) alloys with low As and N compositions (Fig. 8). It is difficult to infer directly from the DOS plots whether the gap would exists for more dilute compositions than those studied here (1.56% of N), but the observed trends suggest that it would. Figure 8 suggests the gap most likely to appear in the alloy containing near 1.56% of N and 3.12% of As (solid red line), because the DOS between the two bands gets to a very low value, yet without a visible flat, zero density region. Increasing nitrogen concentration to 3.12% clearly eliminates the gap. The energies of $\Gamma_v - E_-$ and $\Gamma_v - E_+$ transitions in $\text{GaP}_{0.9532}\text{As}_{0.0312}\text{N}_{0.0156}$ are approximately 1.8 and 2.7 eV, respectively, see Fig. 6(a). The ratio of band gaps (67%) is almost ideal for the IBSC application³². However, the full gap is 0.75 eV above the recommended value of 1.95 eV³². As a result, increased losses due to transmittance of photons with energies below the band gap can negate benefits introduced by the IB. On the other hand this material as an absorber can be integrated in tandem solar cells with the well de-

Electronic band structure of nitrogen diluted Ga(PAsN)

veloped Si-solar cells especially since the lattice mismatch between Si and Ga(PAsN) in this composition regime is almost negligible. Therefore, we are fully convinced that Ga(PAsN) alloy with low N and As concentration is very promising for growth and exploration in the context of solar cell applications.

B. Carrier localization

Spatial localization of electronic states that participate in transport of photogenerated excitations is not desirable and should be assessed when considering new solar cell absorber materials. The fact that incorporation of nitrogen into either GaP or GaAs causes a carrier localization is well known^{68–70}. However, whether the localization changes with different composition of Ga(PAs) alloy as a host has not been discussed so far and only a few papers study the carrier localization in Ga(PAsN)^{20,71}.

In this paper we employ the inverse participation ratio (IPR) as a measure of localization. The IPR for each eigenvalue E_i has been calculated based on the probabilities p_n of finding an electron within a muffin-tin sphere of an atom n ⁴³

$$\text{IPR}(E_i) = \frac{\sum_n p_n^2(E_i)}{[\sum_n p_n(E_i)]^2}. \quad (4)$$

Here the summation index n runs over all atoms in the supercell. Hence, for a 128 atom supercell the IPR may span from 1/128 for an eigenvalue with equal probabilities within the spheres of all atoms, to 1 for an eigenvalue completely confined within a single atomic sphere. More details on the IPR as a measure of localization can be found in⁴³.

The IPR has been calculated for alloys with high P, high As, and nearly 50% of As/P, all with 1.56 and 3.12% of N (Fig. 9). The same property in nitrogen-free host Ga(PAs) alloy has been also calculated for comparison. Further discussion concerning localization will focus on states in vicinity of the band edges that are relevant for transport and optical properties.

States at the band edges of the nitrogen-free Ga(PAs) alloy can be classified as extended since they exhibit a very low IPR [Fig. 9 (a), (b), and (c)]. The compositional disorder mostly affects states located energetically deeper in the VB. The localization-free band edges can be attributed to a close similarity of the alloying elements (P and As) in terms of size and electronegativity and are confirmed experimentally since this material system exhibits narrow low-temperature PL spectra^{72–74}.

Electronic band structure of nitrogen diluted Ga(PAsN)

The situation changes drastically with the introduction of the highly dissimilar nitrogen atom into the system, which has a significantly higher electronegativity and a much smaller atomic radius, see Fig. 9 (d)-(i). In the As-rich limit [Fig. 9 (d)], nitrogen introduces localized *s*-type states at the CB edge which correspond to the energies of the IB. The corresponding orbitals are confined within the second nearest neighbor distance from the nitrogen atoms, see Fig. 10. The increase in nitrogen concentration [Fig. 9 (g)] does not significantly influence the overall character of localization; it lowers slightly and the localized states extend a little into higher energies in the CB. This happens because the higher concentration helps spread the localized states among randomly distributed nitrogen atoms. The behavior might be different in case of nitrogen pairs, triplets and other clusters, however they are not investigated in this study.

The P-rich Ga(PAsN) alloys behaves somewhat differently. The introduction of nitrogen still influences primarily the CB, with even stronger localization due to a slightly higher energy separation from the host conduction band. As a consequence, the localized states spread over a smaller energy range near the band edge [Fig. 9 (f) corresponding to the IB]. However, the localization in the IB reduces significantly with the increase in nitrogen content [Fig. 9 (i)] without any relevant influence on states at the VBE. This behavior differs from the As-rich case due to the different, indirect band-gap character of the host material, where the interaction of nitrogen with the host CB outside of the Γ point of the BZ is higher, and contributes more to the localization processes when the concentration of nitrogen atoms is increased and, therefore, allows for easier delocalization.

IV. SUMMARY

State-of-the-art density functional methods have been used to study the electronic band structure of nitrogen diluted Ga(PAsN) solid solutions to investigate formation of the intermediate band, direct and indirect optical transitions and localization of electronic states. The obtained results have been then confronted with experimental studies of these alloys, further confirming their reliability. The influence of introducing nitrogen to Ga(PAs) host on its electronic band structure has been discussed in terms of its use in optoelectronic devices such as intermediate band solar cells and light emitters. As expected, relatively small amounts of nitrogen introduced to Ga(PAs) allowed for an intermediate nitrogen-related band to appear below the conduction band, but the separation between the intermediate

Electronic band structure of nitrogen diluted Ga(PAsN)

and conduction band may be present for low nitrogen concentrations in P-rich alloys only. In this case the careful analysis of DOS allows us to identify Ga(PAsN) alloys with the energy gap between the IB and the CB (i.e. E_- and E_+ band). Therefore such alloys have been chosen as potential candidates for absorbers suitable for tunable intermediate band solar cells, potentially as the second absorber in Si-based tandem solar cells. In addition, Ga(PAsN) alloys with the global minimum in conduction and intermediate band at the Γ point of Brillouin zone has been identified in our calculations and proposed as potential candidate from group III-V for two colours emitters. It is worth emphasizing that BAC model is insufficient to conclude about the global minimum in the IB and CB since this model works well only near the Γ point of Brillouin zone. In our case calculations of the electronic band structure in whole Brillouin zone allows us to conclude about Ga(PAsN) alloys, which can be potentially useful for two colours emitters. For easy approximation of the electronic band structure at arbitrary P/As and N compositions of Ga(PAsN) and interpretation of experimental results, interpolation formulas have been derived and their parameters gathered in a table. It has been shown that the electronic band structure of Ga(PAsN) is well approximated with the electronic band structures of the highly mismatched ternary dilute nitrides [Ga(PN) and Ga(AsN) in this case] with the same nitrogen concentration used as hosts and then interpolated with the parabolic Vegard equation, commonly used for ordinary semiconductor alloys. In order to improve this interpolation by extending it to the entire Brillouin zone, necessary parameters have been determined and presented in this work. In addition the magnitude of carrier localisation has been calculated, presented as inverse participation ratio and discussed, revealing the highly localized nitrogen states in the intermediate band.

V. ACKNOWLEDGMENTS

This work was supported within the grant of the National Science Centre Poland HARMONIA 2013/10/M/ST3/00638. In addition, M. P. Polak acknowledges the financial support within the MNiSzW “Diamond Grant” no. DI2013 006143. O.R. would like to acknowledge funding provided by the Natural Sciences and Engineering Research Council of Canada under the Discovery Grant Programs RGPIN-2015-04518. All DFT calculations have been performed in Wroclaw Centre of Networking and Supercomputing.

This is the author's peer reviewed, accepted manuscript. However, the online version of record will be different from this version once it has been copyedited and typeset.
PLEASE CITE THIS ARTICLE AS DOI: 10.1063/1.5097977

Electronic band structure of nitrogen diluted Ga(PAsN)

REFERENCES

- ¹W. Shan, W. Walukiewicz, J. Ager III, E. Haller, J. Geisz, D. Friedman, J. Olson, and S. Kurtz, "Band Anticrossing in GaInNAs Alloys," *Physical Review Letters* **82**, 1221–1224 (1999).
- ²A. Lindsay and E. O'Reilly, "Theory of enhanced bandgap non-parabolicity in $\text{GaN}_x\text{As}_{1-x}$ and related alloys," *Solid State Communications* **112**, 443–447 (1999).
- ³P. Kent and A. Zunger, "Evolution of III-V nitride alloy electronic structure: The localized to delocalized transition," *Physical Review Letters* **86**, 2613–2616 (2001).
- ⁴R. Kudrawiec, M. Latkowska, M. Baranowski, J. Misiewicz, L. Li, and J. Harmand, "Photoreflectance, photoluminescence, and microphotoluminescence study of optical transitions between delocalized and localized states in $\text{GaN}_{0.02}\text{As}_{0.98}$, $\text{Ga}_{0.95}\text{In}_{0.05}\text{N}_{0.02}\text{As}_{0.98}$, and $\text{GaN}_{0.02}\text{As}_{0.90}\text{Sb}_{0.08}$ layers," *Physical Review B - Condensed Matter and Materials Physics* **88**, 125201 (2013).
- ⁵S. Bank, H. Bae, L. Goddard, H. Yuen, M. Wistey, R. Kudrawiec, and J. Harris Jr., "Recent progress on 1.55-m dilute-nitride lasers," *IEEE Journal of Quantum Electronics* **43**, 773–785 (2007).
- ⁶M. Gladysiewicz, R. Kudrawiec, and M. Wartak, "Material Gain in $\text{Ga}_{0.341-y}\text{GaN}_y\text{As}_{0.69-y}\text{Sb}_{0.31}$, and $\text{GaN}_y\text{P}_{0.46}\text{Sb}_{0.54-y}$ quantum wells grown on GaAs substrates: Comparative theoretical studies," *IEEE Journal of Quantum Electronics* **50**, 996–1005 (2014).
- ⁷M. Gladysiewicz, R. Kudrawiec, and M. Wartak, "Electronic band structure and material gain of dilute nitride quantum wells grown on InP substrate," *IEEE Journal of Quantum Electronics* **51**, 7056415 (2015).
- ⁸A. Maros, N. Faleev, R. King, and C. Honsberg, "Growth and characterization of $\text{GaAs}_{1-x-y}\text{Sb}_x\text{N}_y/\text{GaAs}$ heterostructures for multijunction solar cell applications," *Journal of Vacuum Science and Technology B: Nanotechnology and Microelectronics* **34**, 02L106 (2016).
- ⁹V. Polojärvi, A. Aho, A. Tukiainen, A. Schramm, and M. Guina, "Comparative study of defect levels in GaInNAs, GaNAsSb, and GaInNAsSb for high-efficiency solar cells," *Applied Physics Letters* **108**, 122104 (2016).
- ¹⁰R. King, D. Bhusari, D. Larrabee, X.-Q. Liu, E. Rehder, K. Edmondson, H. Cotal, R. Jones, J. Ermer, C. Fetzer, D. Law, and N. Karam, "Solar cell generations over 40%

Electronic band structure of nitrogen diluted Ga(PAsN)

- efficiency," *Progress in Photovoltaics: Research and Applications* **20**, 801–815 (2012).
- ¹¹A. Luque and A. Martí, "Increasing the efficiency of ideal solar cells by photon induced transitions at intermediate levels," *Physical Review Letters* **78**, 5014–5017 (1997).
- ¹²A. Luque and A. Martí, "The intermediate band solar cell: Progress toward the realization of an attractive concept," *Advanced Materials* **22**, 160–174 (2010).
- ¹³I. Ramiro, A. Martí, E. Antolín, and A. Luque, "Review of experimental results related to the operation of intermediate band solar cells," *IEEE Journal of Photovoltaics* **4**, 736–748 (2014).
- ¹⁴T. Kada, S. Asahi, T. Kaizu, Y. Harada, T. Kita, R. Tamaki, Y. Okada, and K. Miyano, "Two-step photon absorption in InAs/GaAs quantum-dot superlattice solar cells," *Physical Review B - Condensed Matter and Materials Physics* **91**, 201303 (2015).
- ¹⁵T. Sogabe, Y. Shoji, M. Ohba, K. Yoshida, R. Tamaki, H.-F. Hong, C.-H. Wu, C.-T. Kuo, S. Tomić, and Y. Okada, "Intermediate-band dynamics of quantum dots solar cell in concentrator photovoltaic modules," *Scientific Reports* **4**, 4792 (2014).
- ¹⁶A. Luque, A. Martí, E. Antolín, and C. Tablero, "Intermediate bands versus levels in non-radiative recombination," *Physica B: Condensed Matter* **382**, 320–327 (2006).
- ¹⁷M. Wełna, R. Kudrawiec, Y. Nabetani, T. Tanaka, M. Jaquez, O. Dubon, K. Yu, and W. Walukiewicz, "Effects of a semiconductor matrix on the band anticrossing in dilute group II-VI oxides," *Semiconductor Science and Technology* **30**, 085018 (2015).
- ¹⁸R. Kudrawiec, A. Luce, M. Gladysiewicz, M. Ting, Y. Kuang, C. Tu, O. Dubon, K. Yu, and W. Walukiewicz, "Electronic band structure of $\text{GaN}_x\text{P}_y\text{As}_{1-x-y}$ highly mismatched alloys: Suitability for intermediate-band solar cells," *Physical Review Applied* **1**, 034007 (2014).
- ¹⁹Y. Kuang, K. Yu, R. Kudrawiec, A. Luce, M. Ting, W. Walukiewicz, and C. Tu, "GaNAsP: An intermediate band semiconductor grown by gas-source molecular beam epitaxy," *Applied Physics Letters* **102**, 112105 (2013).
- ²⁰M. Baranowski, R. Kudrawiec, A. V. Luce, M. Latkowska, K. M. Yu, Y. J. Kuang, J. Misiewicz, C. W. Tu, and W. Walukiewicz, "Temperature evolution of carrier dynamics in $\text{GaN}_x\text{P}_y\text{As}_{1-y-x}$ alloys," *Journal of Applied Physics* **117**, 175702 (2015).
- ²¹H. Jussila, P. Kivisaari, J. Lemettinen, T. Tanaka, and M. Sopanen, "Two-Photon Absorption in $\text{GaAs}_{1-x-y}\text{P}_y\text{N}_x$ Intermediate-Band Solar Cells," *Physical Review Applied* **3**, 054007 (2015).

Electronic band structure of nitrogen diluted Ga(PAsN)

- ²²S. Ilahi, S. Almosni, F. Chouchane, M. Perrin, K. Zelazna, N. Yacoubi, R. Kudrawiec, P. Râle, L. Lombez, J.-F. Guillemoles, O. Durand, and C. Cornet, “Optical absorption and thermal conductivity of GaAsPN absorbers grown on GaP in view of their use in multijunction solar cells,” *Solar Energy Materials and Solar Cells* **141**, 291–298 (2015).
- ²³G. Biwa, H. Yaguchi, K. Onabe, and Y. Shiraki, “Photoluminescence and photoluminescence-excitation spectroscopy of GaPAsN/GaP lattice-matched multiple quantum well structures,” *Journal of Crystal Growth* **195**, 574–578 (1998).
- ²⁴C. Robert, A. Bondi, T. Thanh, J. Even, C. Cornet, O. Durand, J. Burin, J. Jancu, W. Guo, A. Létoublon, H. Folliot, S. Boyer-Richard, M. Perrin, N. Chevalier, O. Dehaese, K. Tavernier, S. Loualiche, and A. Le Corre, “Room temperature operation of GaAsP(N)/GaP(N) quantum well based light-emitting diodes: Effect of the incorporation of nitrogen,” *Applied Physics Letters* **98**, 251110 (2011).
- ²⁵A. Babichev, A. Lazarenko, E. Nikitina, E. Pirogov, M. Sobolev, and A. Egorov, “Ultra-wide electroluminescence spectrum of LED heterostructures based on GaPAsN semiconductor alloys,” *Semiconductors* **48**, 501–504 (2014).
- ²⁶K. Zelazna, M. Gladysiewicz, M. P. Polak, S. Almosni, A. Létoublon, C. Cornet, O. Durand, W. Walukiewicz, and R. Kudrawiec, “Nitrogen-related intermediate band in P-rich $\text{GaN}_x\text{P}_y\text{As}_{1-x-y}$ alloys,” *Scientific Reports* **7**, 15703 (2017).
- ²⁷B. Kunert, K. Volz, J. Koch, and W. Stolz, “Direct-band-gap Ga(NAsP)-material system pseudomorphically grown on GaP substrate,” *Applied Physics Letters* **88**, 182108 (2006).
- ²⁸B. Kunert, K. Volz, I. Nemeth, and W. Stolz, “Luminescence investigations of the GaP-based dilute nitride Ga(NAsP) material system,” *Journal of Luminescence* **121**, 361–364 (2006).
- ²⁹S. Liebich, M. Zimprich, A. Beyer, C. Lange, D. Franzbach, S. Chatterjee, N. Hossain, S. Sweeney, K. Volz, B. Kunert, and W. Stolz, “Laser operation of Ga(NAsP) lattice-matched to (001) silicon substrate,” *Applied Physics Letters* **99**, 071109 (2011).
- ³⁰K. Joshi, N. Patel, C. Swarnkar, and U. Paliwal, “Electronic structure of $\text{In}_x\text{Ga}_{1-x}\text{As}_y\text{Sb}_{1-y}$ alloys,” *Computational Materials Science* **49**, S246 – S250 (2010), “Fifth Conference of the Asian Consortium for Computational Materials Science” ” ACCMS-5” ”Hanoi, Vietnam, 9-11 September 2009” ”PROCEEDINGS” .
- ³¹J. Wu, W. Shan, and W. Walukiewicz, “Band anticrossing in highly mismatched III-V semiconductor alloys,” *Semiconductor Science and Technology* **17**, 860 (2002).

Electronic band structure of nitrogen diluted Ga(PAsN)

- ³²A. Luque, A. Martí, and C. Stanley, “Understanding intermediate-band solar cells,” *Nature Photonics* **6**, 146–152 (2012).
- ³³C. Bückers, E. Kühn, C. Schlichenmaier, S. Imhof, A. Thränhardt, J. Hader, J. V. Moloney, O. Rubel, W. Zhang, T. Ackemann, and S. W. Koch, “Quantum modeling of semiconductor gain materials and vertical-external-cavity surface-emitting laser systems,” *Physica Status Solidi (B) Basic Research* **247**, 789–808 (2010).
- ³⁴J. N. Heyman, A. M. Schwartzberg, K. M. Yu, A. V. Luce, O. D. Dubon, Y. J. Kuang, C. W. Tu, and W. Walukiewicz, “Carrier Lifetimes in a III-V-N Intermediate-Band Semiconductor,” *Physical Review Applied* **7**, 014016 (2017).
- ³⁵L. Bellaiche, S.-H. Wei, and A. Zunger, “Composition dependence of interband transition intensities in GaPN, GaAsN, and GaPAs alloys,” *Physical Review B - Condensed Matter and Materials Physics* **56**, 10233–10240 (1997).
- ³⁶P. Kent and A. Zunger, “Theory of electronic structure evolution in GaAsN and GaPN alloys,” *Physical Review B - Condensed Matter and Materials Physics* **64**, 1152081–11520823 (2001).
- ³⁷E. P. O'Reilly, A. Lindsay, and S. Fahy, “Theory of the electronic structure of dilute nitride alloys: beyond the band-anti-crossing model,” *Journal of Physics: Condensed Matter* **16**, S3257 (2004).
- ³⁸J. Neugebauer and C. G. Van de Walle, “Electronic structure and phase stability of $\text{GaAs}_{1-x}\text{N}_x$ alloys,” *Physical Review B - Condensed Matter and Materials Physics* **51**, 10568–10571 (1995).
- ³⁹K. Sakamoto and H. Yaguchi, “First-principles study on the conduction band electron states of GaAsN alloys,” *Physica Status Solidi (C)* **11**, 911–913 (2014).
- ⁴⁰M. Welna, M. Baranowski, W. Linhart, R. Kudrawiec, K. Yu, M. Mayer, and W. Walukiewicz, “Multicolor emission from intermediate band semiconductor $\text{ZnO}_{1-x}\text{Se}_x$,” *Scientific Reports* **7**, 44214 (2017).
- ⁴¹V. Popescu and A. Zunger, “Effective band structure of random alloys,” *Physical Review Letters* **104**, 236403 (2010).
- ⁴²V. Popescu and A. Zunger, “Extracting E versus k - Effective band structure from supercell calculations on alloys and impurities,” *Physical Review B - Condensed Matter and Materials Physics* **85**, 085201 (2012).
- ⁴³C. Pashartis and O. Rubel, “Localization of Electronic States in III-V Semiconductor Alloys: A Comparative Study,” *Physical Review Applied* **7**, 064011 (2017).

Electronic band structure of nitrogen diluted Ga(PAsN)

- ⁴⁴P. Hohenberg and W. Kohn, "Inhomogeneous Electron Gas," Physical Review **136**, B864–B871 (1964).
- ⁴⁵W. Kohn and L. J. Sham, "Self-Consistent Equations Including Exchange and Correlation Effects," Physical Review **140**, A1133–A1138 (1965).
- ⁴⁶P. Blaha, K. Schwarz, G. K. H. Madsen, D. Kvasnicka, J. Luitz, R. Laskowski, F. Tran, and L. D. Marks, *WIEN2k, An Augmented Plane Wave + Local Orbitals Program for Calculating Crystal Properties* (Karlheinz Schwarz, Techn. Universität Wien, Austria, 2001).
- ⁴⁷J. Sun, R. C. Remsing, Y. Zhang, Z. Sun, A. Ruzsinszky, H. Peng, Z. Yang, A. Paul, U. Waghmare, X. Wu, M. L. Klein, and J. P. Perdew, "Accurate first-principles structures and energies of diversely bonded systems from an efficient density functional," Nature Chemistry **8**, 831 (2016).
- ⁴⁸F. Tran and P. Blaha, "Accurate band gaps of semiconductors and insulators with a semilocal exchange-correlation potential," Physical Review Letters **102**, 226401 (2009).
- ⁴⁹J. Perdew and Y. Wang, "Accurate and simple analytic representation of the electron-gas correlation energy," Physical Review B - Condensed Matter and Materials Physics **45**, 13244–13249 (1992).
- ⁵⁰K. B. Joshi, U. Paliwal, and B. K. Sharma, "Hybrid functionals and electronic structure of high-pressure phase of CdO," physica status solidi (b) **248**, 1248–1252 (2011).
- ⁵¹D. Koller, F. Tran, and P. Blaha, "Merits and limits of the modified Becke-Johnson exchange potential," Physical Review B - Condensed Matter and Materials Physics **83**, 195134 (2011).
- ⁵²Y.-S. Kim, M. Marsman, G. Kresse, F. Tran, and P. Blaha, "Towards efficient band structure and effective mass calculations for III-V direct band-gap semiconductors," Physical Review B - Condensed Matter and Materials Physics **82**, 205212 (2010).
- ⁵³J. Camargo-Martínez and R. Baquero, "Performance of the modified Becke-Johnson potential for semiconductors," Physical Review B - Condensed Matter and Materials Physics **86**, 195106 (2012).
- ⁵⁴A. Zunger, S.-H. Wei, L. Ferreira, and J. Bernard, "Special quasirandom structures," Physical Review Letters **65**, 353–356 (1990).
- ⁵⁵A. Van De Walle, P. Tiwary, M. De Jong, D. Olmsted, M. Asta, A. Dick, D. Shin, Y. Wang, L.-Q. Chen, and Z.-K. Liu, "Efficient stochastic generation of special quasirandom structures," Calphad: Computer Coupling of Phase Diagrams and Thermochemistry **42**, 13–18 (2013).

Electronic band structure of nitrogen diluted Ga(PAsN)

- ⁵⁶H. J. Monkhorst and J. D. Pack, "Special points for Brillouin-zone integrations," Physical Review B - Condensed Matter and Materials Physics **13**, 5188–5192 (1976).
- ⁵⁷M. Landmann, E. Rauls, W. G. Schmidt, M. Röppischer, C. Cobet, N. Esser, T. Schupp, D. J. As, M. Feneberg, and R. Goldhahn, "Transition energies and direct-indirect band gap crossing in zinc-blende $\text{Al}_x\text{Ga}_{1-x}\text{N}$," Phys. Rev. B **87**, 195210 (2013).
- ⁵⁸M. P. Polak, P. Scharoch, and R. Kudrawiec, "The electronic band structure of $\text{Ge}_{1-x}\text{Sn}_x$ in the full composition range: indirect, direct, and inverted gaps regimes, band offsets, and the Burstein-Moss effect," Journal of Physics D: Applied Physics **50**, 195103 (2017).
- ⁵⁹P. Blöchl, O. Jepsen, and O. Andersen, "Improved tetrahedron method for Brillouin-zone integrations," Physical Review B - Condensed Matter and Materials Physics **49**, 16223–16233 (1994).
- ⁶⁰O. Rubel, A. Bokhanchuk, S. Ahmed, and E. Assmann, "Unfolding the band structure of disordered solids: From bound states to high-mobility Kane fermions," Physical Review B - Condensed Matter and Materials Physics **90**, 115202 (2014).
- ⁶¹I. Vurgaftman, J. R. Meyer, and L. R. Ram-Mohan, "Band parameters for III-V compound semiconductors and their alloys," Journal Applied Physics **80**, 5815 (2001).
- ⁶²W. A. Harrison, *Electronic structure and the properties of solids: the physics of the chemical bond.* (San Francisco: Freeman, 1980).
- ⁶³K. A. Mäder and A. Zunger, "Short- and long-range-order effects on the electronic properties of iii-v semiconductor alloys," Phys. Rev. B **51**, 10462–10476 (1995).
- ⁶⁴J. Wu, W. Walukiewicz, K. M. Yu, J. W. Ager, E. E. Haller, Y. G. Hong, H. P. Xin, and C. W. Tu, "Band anticrossing in $\text{GaP}_{1-x}\text{N}_x$ alloys," Physical Review B - Condensed Matter and Materials Physics **65**, 2413031–2413034 (2002).
- ⁶⁵P. R. C. Kent and A. Zunger, "Nitrogen pairs, triplets, and clusters in GaAs and GaP," Applied Physics Letters **79**, 2339 (2001).
- ⁶⁶W. Shan, W. Walukiewicz, K. M. Yu, J. Wu, J. W. Ager, E. E. Haller, H. P. Xin, and C. W. Tu, "Nature of the fundamental band gap in $\text{GaN}_x\text{P}_{1-x}$ alloys," Applied Physics Letters **76**, 3251–3253 (2000).
- ⁶⁷W. Shan, W. Walukiewicz, J. W. Ager, E. E. Haller, J. F. Geisz, D. J. Friedman, J. M. Olson, and S. R. Kurtz, "Band Anticrossing in GaInNAs Alloys," Applied Physics Letters **82**, 1221–1224 (1999).
- ⁶⁸I. Buyanova, W. Chen, and C. Tu, "Recombination processes in N-containing III-V ternary alloys," Solid-State Electronics **47**, 467 – 475 (2003).

Electronic band structure of nitrogen diluted Ga(PAsN)

- ⁶⁹R. Kudrawiec, G. Sek, J. Misiewicz, L. H. Li, and J. C. Harmand, "Influence of carrier localization on modulation mechanism in photoreflectance of GaAsN and GaInAsN," *Applied Physics Letters* **83**, 1379–1381 (2003).
- ⁷⁰R. Kudrawiec, M. Latkowska, M. Baranowski, J. Misiewicz, L. H. Li, and J. C. Harmand, "Photoreflectance, photoluminescence, and microphotoluminescence study of optical transitions between delocalized and localized states in $\text{GaN}_{0.02}\text{As}_{0.98}$, $\text{Ga}_{0.95}\text{In}_{0.05}\text{N}_{0.02}\text{As}_{0.98}$, and $\text{GaN}_{0.02}\text{As}_{0.90}\text{Sb}_{0.08}$ layers," *Physical Review B - Condensed Matter and Materials Physics* **88**, 125201 (2013).
- ⁷¹R. Woscholski, S. Gies, M. Wiemer, M. K. Shakfa, A. Rahimi-Iman, P. Ludewig, S. Reinhard, K. Jandieri, S. D. Baranovskii, W. Heimbrodt, K. Volz, W. Stolz, and M. Koch, "Influence of growth temperature and disorder on spectral and temporal properties of Ga(NAsP) heterostructures," *Journal of Applied Physics* **119**, 145707 (2016).
- ⁷²S. Lai and M. V. Klein, "Evidence for Exciton Localization by Alloy Fluctuations in Indirect-Gap $\text{GaAs}_x\text{P}_{1-x}$," *Applied Physics Letters* **44**, 1087–1090 (1980).
- ⁷³M. Oueslatii, C. B. B. L. Guillaume, and M. Zouaghitb, "Calculated emission intensity band M0 from localised states due to disorder in $\text{GaAs}_{1-x}\text{P}_x$, alloys," *Journal of Physics: Condensed Matter* **1**, 7705–7714 (1989).
- ⁷⁴A. Fried, A. Ron, and E. Cohen, "Intrinsic exciton states in indirect-band-gap $\text{GaAs}_x\text{P}_{1-x}$: Composition dependence and effects of impurities," *Physical Review B - Condensed Matter and Materials Physics* **39**, 5913–5918 (1989).

Electronic band structure of nitrogen diluted Ga(PAsN)

TABLE I. Calculated and experimental⁶¹ values of band gaps and lattice constants a for parent zinc-blend binary compounds; c is the adjusted mBJLDA parameter. All values correspond to 0 K temperature except for GaN where the experimental value of $a = 4.5 \text{ \AA}$ corresponds to 300 K.

Property	GaP		GaAs		GaN	
	$(c = 1.50)$		$(c = 1.53)$		$(c = 2.10)$	
	DFT	Exp.	DFT	Exp.	DFT	Exp.
Direct gap (eV)	2.89	2.89	1.52	1.52	3.30	3.30
Indirect gap (eV)	2.33 (X)	2.35 (X)	1.72 (L)	1.81 (L)	4.99 (X)	4.52 (X)
a (\AA)	5.48	5.45	5.68	5.65	4.46	4.5

This is the author's peer reviewed, accepted manuscript. However, the online version of record will be different from this version once it has been copyedited and typeset.
PLEASE CITE THIS ARTICLE AS DOI: 10.1063/1.5097977

Electronic band structure of nitrogen diluted Ga(PAsN)

TABLE II. Parameters used in description of composition-dependent band gap of the studied alloys.

Eq	Transition	Parameter	GaP _{1-x} As _x	GaP _{1-x} N _x	GaAs _{1-x} N _x	GaP _{1-x-y} As _x N _y
(2)	$\Gamma_V - \Gamma_C$	b (eV)	0.33	—	—	0.33
		E_{AB} (eV)	2.87	—	—	$\frac{1}{2} \left(2.87 + 2.18 \pm \sqrt{(2.87 - 2.18)^2 + 4 \cdot 3.05^2 y} \right)$
		E_{AC} (eV)	1.52	—	—	$\frac{1}{2} \left(1.52 + 1.65 \pm \sqrt{(1.52 - 1.65)^2 + 4 \cdot 2.7^2 y} \right)$
	$\Gamma_V - L_C$	b (eV)	0.31	—	—	0.31
		E_{AB} (eV)	2.5	—	—	$\frac{1}{2} \left(2.5 + 2.18 + \sqrt{(2.5 - 2.18)^2 + 4 \cdot 1.65^2 y} \right)$
		E_{AC} (eV)	1.72	—	—	$\frac{1}{2} \left(1.72 + 1.65 + \sqrt{(1.72 - 1.65)^2 + 4 \cdot 0.85^2 y} \right)$
(3)	$\Gamma_V - X_C$	b (eV)	0.32	—	—	0.32
		E_{AB} (eV)	2.33	—	—	$\frac{1}{2} \left(2.33 + 2.18 + \sqrt{(2.33 - 2.18)^2 + 4 \cdot 0.97^2 y} \right)$
		E_{AC} (eV)	1.99	—	—	$\frac{1}{2} \left(1.99 + 1.65 + \sqrt{(1.99 - 1.65)^2 + 4 \cdot 0.68^2 y} \right)$
	$E_{\pm}(\Gamma)$	$E_M(\Gamma)$ (eV)	—	2.87	1.52	—
		$C_{NM}(\Gamma)$ (eV)	—	3.05	2.7	—
		$E_+(L)$	$E_M(L)$ (eV)	—	2.5	1.72
	$E_+(X)$	$C_{NM}(L)$ (eV)	—	1.65	0.85	—
		$E_M(X)$ (eV)	—	2.33	1.99	—
		$C_{NM}(X)$ (eV)	—	0.97	0.68	—
		E_N (eV)	—	2.18	1.65	—

Electronic band structure of nitrogen diluted Ga(PAsN)

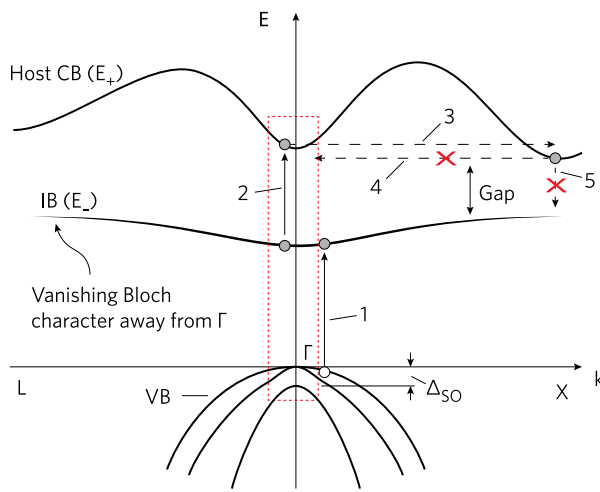


FIG. 1. Schematic band structure illustrating important ingredients and relevant processes in an intermediate band (IB) solar cell material of Ga(PAsN) family: 1 – primary excitation, 2 – secondary excitation, 3 – scattering from Γ to X valley, 4 – backscattering, and 5 – re-trapping. The direct excitation from the valence band (VB) to the host conduction band (CB) is not shown for simplicity. The dotted red line shows a region of applicability for a combined $\mathbf{k}\cdot\mathbf{p}$ and BAC model.

This is the author's peer reviewed, accepted manuscript. However, the online version of record will be different from this version once it has been copyedited and typeset.
 PLEASE CITE THIS ARTICLE AS DOI: 10.1063/1.5097977

Electronic band structure of nitrogen diluted Ga(PAsN)

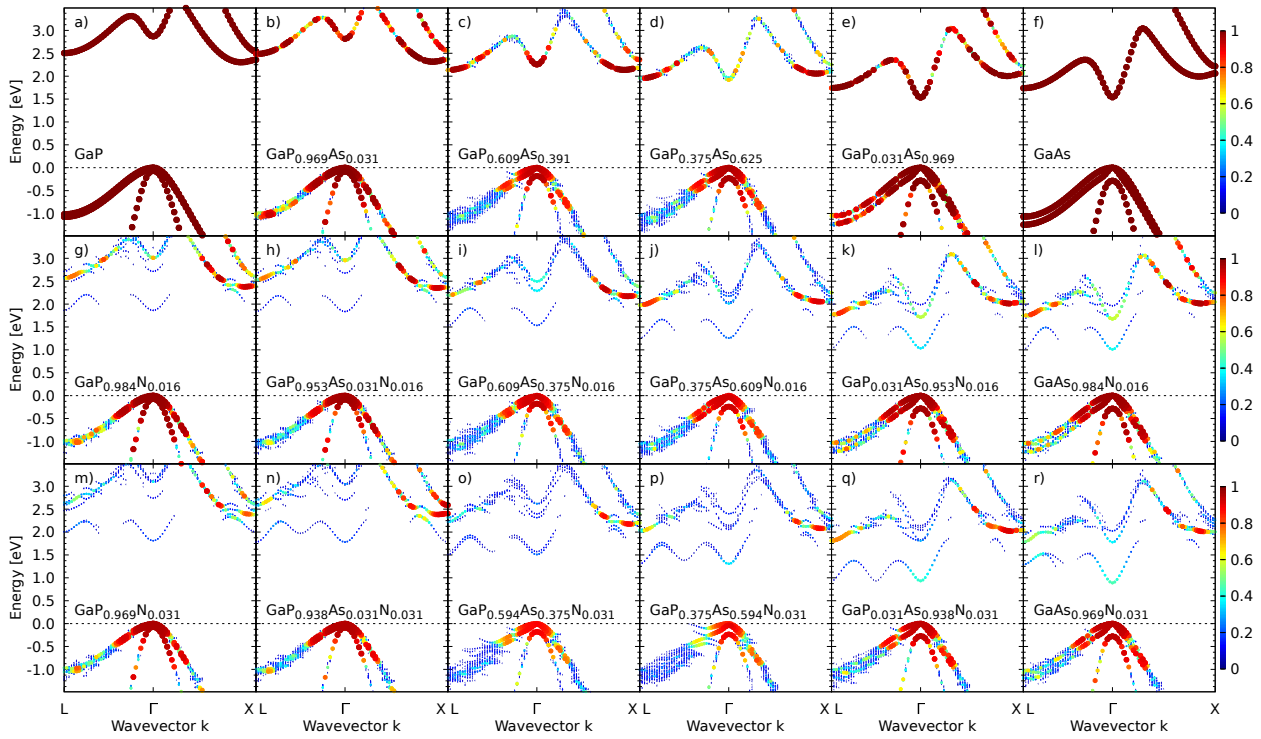


FIG. 2. Unfolded band structures of all the studied alloys organized row- and column-wise. P/As ratio changes from left to right (As increases), nitrogen concentration increases from top to bottom.

Electronic band structure of nitrogen diluted Ga(PAsN)

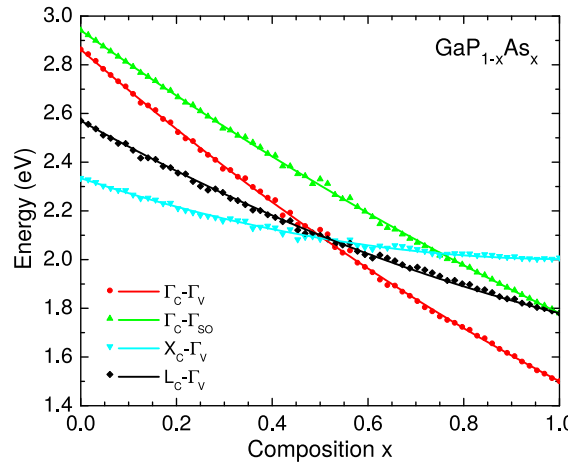


FIG. 3. Direct ($\Gamma_v - \Gamma_c$) and indirect ($\Gamma_v - L_c$ and $\Gamma_v - X_c$) band gaps in the host $\text{GaP}_{1-x}\text{As}_x$ alloy as a function of As concentration. The points represent results from DFT calculations while the curves are fitted with Eq. (2) using parameters listed in Table II.

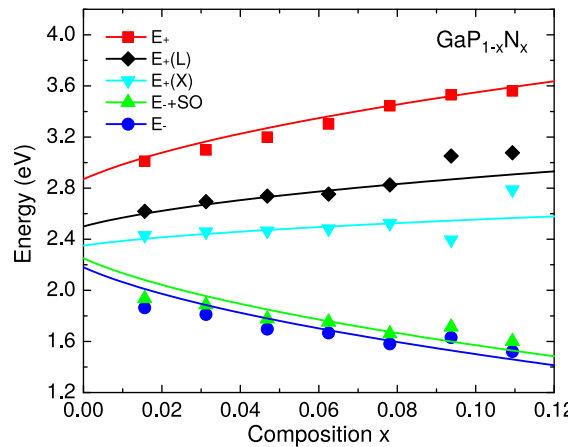


FIG. 4. Direct ($\Gamma - E_-$ and ($\Gamma - E_+$)) and indirect ($\Gamma - E_+(X)$ and $\Gamma - E_+(L)$) band gaps in the $\text{GaP}_{1-x}\text{N}_x$ alloy as a function of N concentration. The points represent results of DFT calculations while the curves are fitted with Eq. (3) using parameters listed in Table II.

Electronic band structure of nitrogen diluted Ga(PAsN)

This is the author's peer reviewed, accepted manuscript. However, the online version of record will be different from this version once it has been copyedited and typeset.
 PLEASE CITE THIS ARTICLE AS DOI: 10.1063/1.5097977

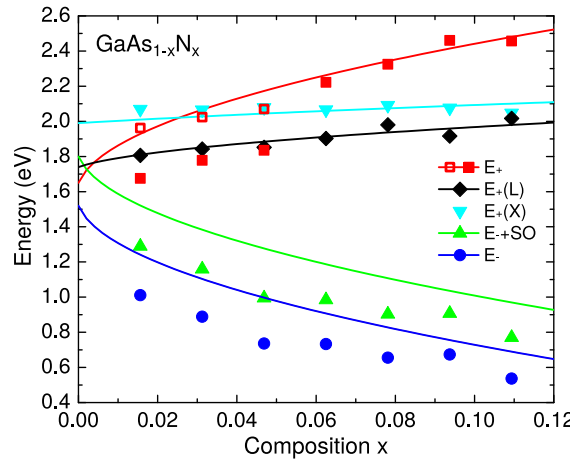


FIG. 5. Direct (Γ - E_- and Γ - E_+) and indirect (Γ - $E_+(X)$ and Γ - $E_+(L)$) band gaps in the $\text{GaAs}_{1-x}\text{N}_x$ alloy as a function of N concentration. The points represent results from DFT calculations while the curves are fitted with Eq. (3) using parameters listed in Table II.

This is the author's peer reviewed, accepted manuscript. However, the online version of record will be different from this version once it has been copyedited and typeset.
 PLEASE CITE THIS ARTICLE AS DOI: 10.1063/1.5097977

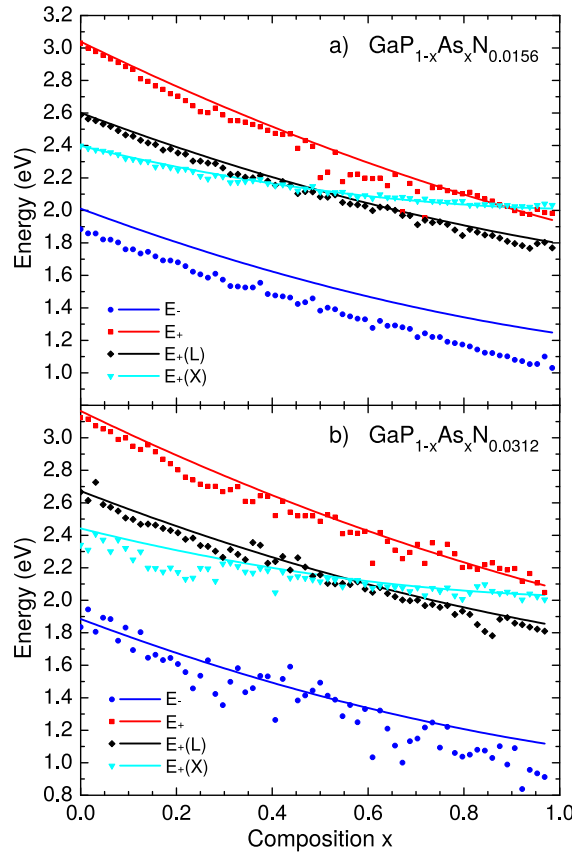


FIG. 6. Direct (Γ - E_- and Γ - E_+) and indirect (Γ - $E_+(X)$ and Γ - $E_+(L)$) band gaps in the $\text{GaP}_{1-x-y}\text{As}_x\text{N}_y$ alloy as a function of As concentration, with the fixed nitrogen content of (a) 1.56% and (b) 3.12%. The points represent results from DFT calculations while the curves are fitted with Eq. (2) using parameters listed in Table II.

Electronic band structure of nitrogen diluted Ga(PAsN)

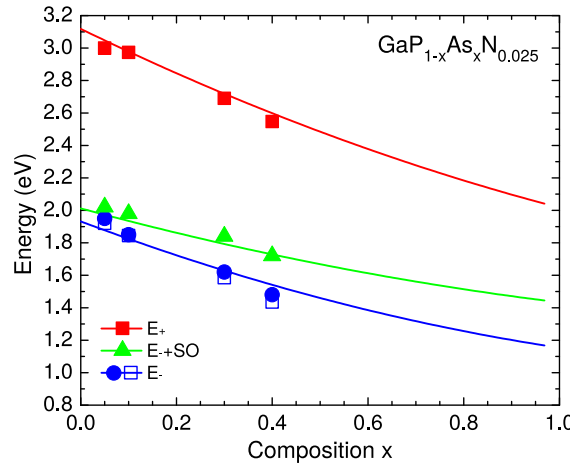


FIG. 7. Direct band gap transitions $\Gamma - E_-$, $\Gamma - E_+$, and the split-off band transition ($\Gamma_{SO} - E_-$) in the Ga(PAsN) alloy as a function of As concentration. Solid points represent modulated transmittance results, open points are results of photoreflectance spectroscopy, both from Ref.²⁶ where the nitrogen content has been determined to be around 2.5%, although with high uncertainty. The lines are the fitted curves from our calculations (Eq. (3) with parameters from Table II).

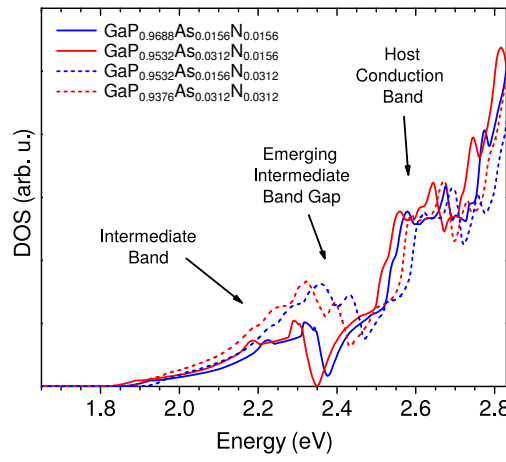


FIG. 8. Density of states for different As and N concentration. Solid and dashed lines correspond to 1.56% and 3.12% of nitrogen respectively, blue and red lines correspond to 1.56% and 3.12% of arsenic respectively.

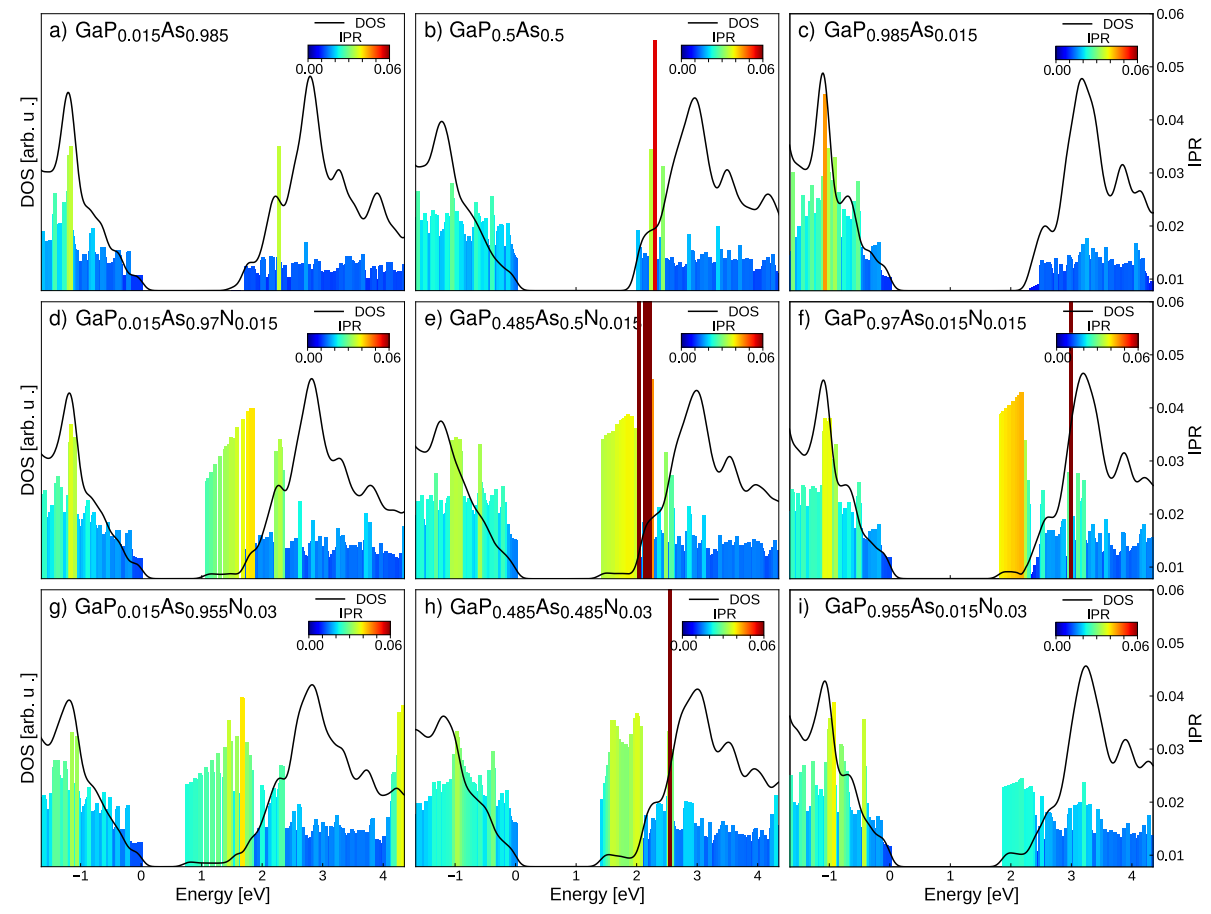


FIG. 9. Density of states (DOS) and spectrally-resolved inverse participation ratio (IPR) for states in vicinity of the band edges.

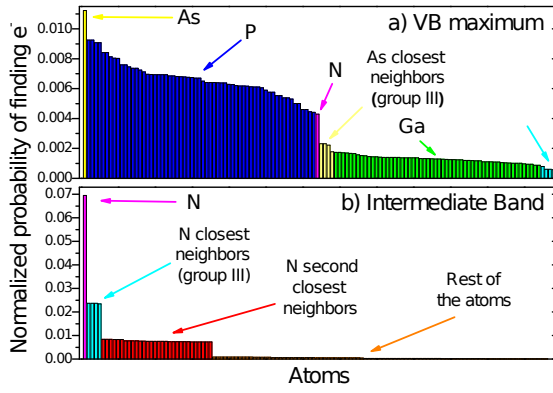


FIG. 10. The localization of carriers in $\text{GaP}_{0.9688}\text{As}_{0.0156}\text{N}_{0.0156}$ represented as a normalized probability of finding an electron within the sphere of each atom in descending order from left to right. Probabilities for (a) the top of the valence band and (b) the bottom of the intermediate band.